

NT@UW-02-034

Relativity, chiral symmetry, and the nucleon electromagnetic form factors

Gerald A. Miller

University of Washington Seattle, WA 98195-1560

December 22, 2018

Abstract

A relativistic interpretation for why the proton’s G_E/G_M falls and QF_2/F_1 is approximately constant is presented. Reproducing the observed G_E^n mandates the inclusion of the effects of the pion cloud. The full relativistic model with a pion cloud provides a good reproduction of all of the nucleon electromagnetic form factors.

1 Introduction

An alternate title could be “Surprises in the Proton”. This talk owes its existence to the precise, stunning and exciting recent experimental work on measuring G_E/G_M (or QF_2/F_1) for the proton and G_E, G_M for the neutron. My goal here is to interpret the data. Symmetries including Poincaré invariance and chiral symmetry will be the principal tool I’ll use. This talk is based on three papers [1],[2],[3].

If, a few years ago, one had asked participants at a meeting like this about the Q^2 dependence of the proton’s G_E/G_M or QF_2/F_1 . Almost everyone one have answered that for large enough values of Q^2 , G_E/G_M would be flat and QF_2/F_1 would fall with increasing Q^2 . The reason for the latter fall being conservation of hadron helicity. Indeed, the shapes of the curves have been obtained in the new measurements, except for the mis-labeling of the ordinate axes. The expected flatness of G_E/G_M holds for QF_2/F_1 , and the

quantity G_E/G_M falls rapidly and linearly with Q^2 . This behavior needs to be understood!

2 Outline

I will begin with a brief introduction to Light Front Physics. Then I will discuss a particular relativistic model of the nucleon, and proceed to apply it to the proton form factors, with the aim of providing a qualitative understanding of the salient experimental features. The same model fails to reproduce the neutron G_E unless the effects of the pion cloud are included. The combination of relativistic effects with those of the pion cloud lead to a model that is able to reproduce all of the nucleon electromagnetic form factors.

3 Light Front

Light-front dynamics is a relativistic many-body dynamics in which fields are quantized at a “time” = $\tau = x^0 + x^3 \equiv x^+$. The τ -development operator is then given by $P^0 - P^3 \equiv P^-$. These equations show the notation that a four-vector A^μ is expressed as $A^\pm \equiv A^0 \pm A^3$. One quantizes at $x^+ = 0$ which is a light-front, hence the name “light front dynamics”. The canonical spatial variable must be orthogonal to the time variable, and this is given by $x^- = x^0 - x^3$. The canonical momentum is then $P^+ = P^0 + P^3$. The other coordinates are \mathbf{x}_\perp and \mathbf{P}_\perp .

The most important consequence of this is that the relation between energy and momentum of a free particle is given by: $p_\mu p^\mu = m^2 = p^+ p^- - p_\perp^2 \rightarrow p^- = \frac{p_\perp^2 + m^2}{p^+}$, a relativistic kinetic energy which does not contain a square root operator. This allows the separation of center of mass and relative coordinates, so that the computed wave functions are frame independent.

The use of the light front is particularly relevant for calculating form factors, which are probability amplitudes for an nucleon to absorb a four momentum q and remain a nucleon. The initial and final nucleons have different total momenta. This means that the final nucleon is a boosted nucleon, with different wave function than the initial nucleon. In general, performing the boost is difficult for large values of $Q^2 = -q^2$. However the light front technique allows one to set up the calculation so that the boosts

are independent of interactions. Indeed, the wave functions are functions of relative variables and are independent of frame.

4 Definitions

Let us define the basic quantities concerning us here. These are the independent form factors defined by

$$\langle N, \lambda' p' | J^\mu | N, \lambda p \rangle = \bar{u}_{\lambda'}(p') \left[F_1(Q^2) \gamma^\mu + \frac{\kappa F_2(Q^2)}{2M_N} i\sigma^{\mu\nu} (p' - p)_\nu \right] u_\lambda(p). \quad (1)$$

The Sachs form factors are defined by the equations:

$$G_E = F_1 - \frac{Q^2}{4M_N^2} \kappa F_2, \quad G_M = F_1 + \kappa F_2. \quad (2)$$

There is an alternate light front interpretation, based on field theory, in which one uses the “good” component of the current, J^+ , to suppress the effects of quark-pair terms. Then, using nucleon light-cone spinors:

$$F_1(Q^2) = \frac{1}{2P^+} \langle N, \uparrow | J^+ | N, \uparrow \rangle, \quad Q\kappa F_2(Q^2) = \frac{-2M_N}{2P^+} \langle N, \uparrow | J^+ | N, \downarrow \rangle. \quad (3)$$

The form factor F_1 is obtained from the non-spin flip matrix element, while F_2 is obtained from the spin-flip term.

5 Three-Body Variables and Boost

We use light front coordinates for the momentum of each of the i quarks, such that $\mathbf{p}_i = (p_i^+, \mathbf{p}_{i\perp}), p^- = (p_\perp^2 + m^2)/p^+$. The total (perp)-momentum is $\mathbf{P} = \mathbf{p}_1 + \mathbf{p}_2 + \mathbf{p}_3$, the plus components of the momenta are denoted as

$$\xi = \frac{p_1^+}{p_1^+ + p_2^+}, \quad \eta = \frac{p_1^+ + p_2^+}{P^+}, \quad (4)$$

and the perpendicular relative coordinates are given by

$$\mathbf{k}_\perp = (1 - \xi)\mathbf{p}_{1\perp} - \xi\mathbf{p}_{2\perp}, \quad \mathbf{K}_\perp = (1 - \eta)(\mathbf{p}_{1\perp} + \mathbf{p}_{2\perp}) - \eta\mathbf{p}_{3\perp}. \quad (5)$$

In the center of mass frame we find:

$$\mathbf{p}_{1\perp} = \mathbf{k}_{\perp} + \xi \mathbf{K}_{\perp}, \quad \mathbf{p}_{2\perp} = -\mathbf{k}_{\perp} + (1 - \xi) \mathbf{K}_{\perp}, \quad \mathbf{p}_{3\perp} = -\mathbf{K}_{\perp}. \quad (6)$$

The coordinates $\xi, \eta, \mathbf{k}, \mathbf{K}$ are all relative coordinates so that one obtains a frame independent wave function $\Psi(\mathbf{k}_{\perp}, \mathbf{K}_{\perp}, \xi, \eta)$.

Now consider the computation of a form factor, taking quark 3 to be the one struck by the photon. One works in a special set of frames with $q^+ = 0$ and $Q^2 = \mathbf{q}_{\perp}^2$, so that the value of $1 - \eta$ is not changed by the photon. The coordinate $\mathbf{p}_{3\perp}$ is changed to $\mathbf{p}_{3\perp} + \mathbf{q}_{\perp}$, so only one relative momentum, \mathbf{K}_{\perp} is changed:

$$\mathbf{K}'_{\perp} = (1 - \eta)(\mathbf{p}_{1\perp} + \mathbf{p}_{2\perp}) - \eta(\mathbf{p}_{3\perp} + \mathbf{q}_{\perp}) = \mathbf{K}_{\perp} - \eta \mathbf{q}_{\perp}, \quad \mathbf{k}'_{\perp} = \mathbf{k}_{\perp}, \quad (7)$$

The arguments of the spatial wave function are taken as the mass-squared operator for a non-interacting system:

$$M_0^2 \equiv \sum_{i=1,3} p_i^- P^+ - P_{\perp}^2 = \frac{K_{\perp}^2}{\eta(1 - \eta)} + \frac{k_{\perp}^2 + m^2}{\eta \xi(1 - \xi)} + \frac{m^2}{1 - \eta}. \quad (8)$$

This is a relativistic version of the square of the center-of-mass kinetic energy, expressed in terms of light-front variables. Note that the absorption of a photon changes the value to:

$$M_0'^2 = \frac{(K_{\perp} - \eta q_{\perp})^2}{\eta(1 - \eta)} + \frac{k_{\perp}^2 + m^2}{\eta \xi(1 - \xi)} + \frac{m^2}{1 - \eta}. \quad (9)$$

6 Wave function

Our wave function is based on symmetries. The wave function is anti-symmetric, a function of relative momenta, independent of reference frame, an eigenstate of the spin operator and rotationally invariant (in a specific well-defined sense). The use of symmetries is manifested in the construction of such wave functions, as originally described by Terent'ev [4], Coester[5] and their collaborators. A schematic form of the wave function is

$$\Psi(p_i) = \Phi(M_0^2) u(p_1) u(p_2) u(p_3) \psi(p_1, p_2, p_3), \quad p_i = \mathbf{p}_i s_i, \tau_i \quad (10)$$

where ψ is a spin-isospin color amplitude factor, the p_i are expressed in terms of relative coordinates (for example, $\mathbf{p}_{3\perp} = -\mathbf{K}_{\perp}$), the $u(p_i)$ are ordinary

Dirac spinors and Φ is a spatial wave function. The ordinary Dirac spinors depend on the third or z component of the momenta and this is given, for example, by $p_{3z} = \frac{1}{2}[M_0(1 - \eta) - \frac{m^2 + K_\perp^2}{(1 - \eta)M_0}]$.

We take the the spatial wave function from Schlumpf[6]:

$$\Phi(M_0) = \frac{N}{(M_0^2 + \beta^2)^\gamma}, \beta = 0.607 \text{ GeV}, \gamma = 3.5, m = 0.267 \text{ GeV}. \quad (11)$$

The value of γ is chosen that $Q^4 G_M(Q^2)$ is approximately constant for $Q^2 > 4 \text{ GeV}^2$ in accord with experimental data. The parameter β helps govern the values of the perp-momenta allowed by the wave function Φ and is closely related to the rms charge radius, and m is mainly determined by the magnetic moment of the proton.

At this point the wave function and the calculation are completely defined. One could evaluate the form factors as $\langle \Psi | J^+ | \Psi \rangle$ and obtain the results. Actually the first results were obtained in 1995[1], and are given as Figs. 10,11 in that reference. It is clear that the model predicted that G_E falls off much more rapidly with increasing Q^2 than does G_M . The result that $Q^4 G_M$ is flat at high Q^2 is a consequence of using Schlumpf's wave function, but our values of G_E for large Q^2 were a prediction.

So we had this early prediction, which was confirmed by experimental measurements. But we didn't present an explanation of the numerical results. This is the next task.

7 Simplify Calculation- Light Cone Spinors

The evaluation of the operator $J^+ \sim \gamma^+$ is simplified by using light cone spinors. These solutions of the free Dirac equation, related to ordinary Dirac spinors by a unitary transformation, conveniently satisfy:

$$\bar{u}_L(p^+, \mathbf{p}', \lambda') \gamma^+ u_L(p^+, \mathbf{p}, \lambda) = 2\delta_{\lambda\lambda'} p^+. \quad (12)$$

To take advantage of this, re-express the wave function in terms of light-front spinors using the completeness relation: $1 = \sum_{\lambda} u_L(p, \lambda) \bar{u}_L(p, \lambda)$. We then find

$$\Psi(p_i) = u_L(p_1, \lambda_1) u_L(p_2, \lambda_2) u_L(p_3, \lambda_3) \psi_L(p_i, \lambda_i), \quad (13)$$

$$\begin{aligned} \psi_L(p_i, \lambda_i) &\equiv [\bar{u}_L(\mathbf{p}_1, \lambda_1) u(\mathbf{p}_1, s_1)] [\bar{u}_L(\mathbf{p}_2, \lambda_2) u(\mathbf{p}_2, s_2)] \\ &\times [\bar{u}_L(\mathbf{p}_3, \lambda_3) u(\mathbf{p}_3, s_3)] \psi(p_1, p_2, p_3). \end{aligned} \quad (14)$$

This is the very same Ψ as before, it is just that now it is easy to compute the matrix elements of the γ^+ operator.

The unitary transformation is also known as the Melosh rotation. The basic point is that one may evaluate the coefficients in terms of Pauli spinors: $|\lambda_i\rangle, |s_i\rangle$, with $\langle\lambda_i|R_M^\dagger(\mathbf{p}_i)|s_i\rangle \equiv \bar{u}_L(\mathbf{p}_i, \lambda_i)u(\mathbf{p}_i, s_i)$. It is easy to show that

$$\langle\lambda_3|R_M^\dagger(\mathbf{p}_3)|s_3\rangle = \langle\lambda_3|\left[\frac{m + (1 - \eta)M_0 + i\boldsymbol{\sigma} \cdot (\mathbf{n} \times \mathbf{p}_3)}{\sqrt{(m + (1 - \eta)M_0)^2 + p_{3\perp}^2}}\right]|s_3\rangle. \quad (15)$$

The important effect resides in the term $(\mathbf{n} \times \mathbf{p}_3)$ which originates from the lower components of the Dirac spinors. This large relativistic spin effect can be summarized: the effects of relativity are to replace Pauli spinors by Melosh rotation operators acting on Pauli spinors. Thus

$$|\uparrow \mathbf{p}_i\rangle \equiv R_M^\dagger(\mathbf{p}_i) \begin{pmatrix} 1 \\ 0 \end{pmatrix}, \quad |\uparrow \mathbf{p}_3\rangle \neq |\uparrow\rangle. \quad (16)$$

In the non-relativistic limit, the Melosh rotation matrices become unit operators and one recovers the familiar $SU(6)$ quark model.

8 Proton F_1, F_2 -Analytic Insight

The analytic insight is based on Eq. (15). Consider high momentum transfer such that $Q = \sqrt{\mathbf{q}_\perp^2} \gg \beta = 560$ MeV. Each of the quantities: $M_0, M'_0, \mathbf{p}_{3\perp}, \mathbf{p}_{3\perp}$ can be of order q_\perp , so the spin-flip term is as large as the non-spin flip term. In particular, ($s_3 = +1/2$) may correspond to ($\lambda_3 = -1/2$), so the spin of the struck quark \neq proton spin. This means that there is no hadron helicity selection rule[7, 8].

The effects of the lower components of Dirac spinors, which cause the spin flip term $\boldsymbol{\sigma} \times \mathbf{p}_3$, are the same as having a non-zero L_z , if the wave functions are expressed in the light-front basis.

We may now qualitatively understand the numerical results, since

$$F_1(Q^2) = \int \frac{d^2q_\perp d\xi}{\xi(1 - \xi)} \frac{d^2K_\perp d\eta}{\eta(1 - \eta)} \cdots \langle \uparrow \mathbf{p}'_3 | \uparrow \mathbf{p}_3 \rangle \quad (17)$$

$$Q\kappa F_2(Q^2) = 2M_N \int \frac{d^2q_\perp d\xi}{\xi(1 - \xi)} \frac{d^2K_\perp d\eta}{\eta(1 - \eta)} \cdots \langle \uparrow \mathbf{p}'_3 | \downarrow \mathbf{p}_3 \rangle, \quad (18)$$

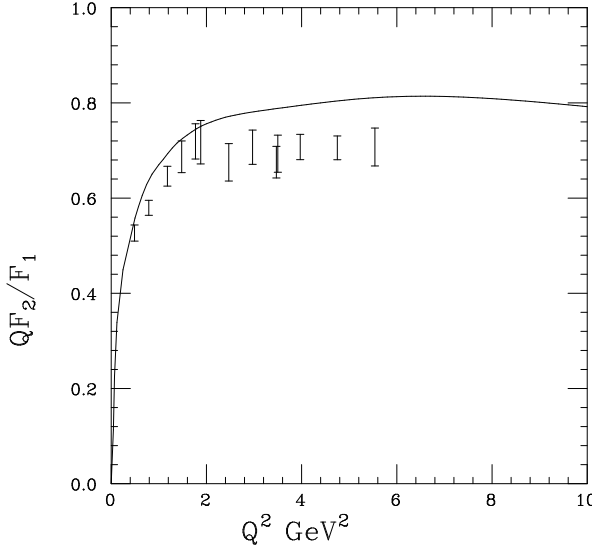


Figure 1: Calculation of Refs. [1, 2], data are from Jones *et al.*[9] for $2 \leq Q^2 \leq 3.5 \text{ GeV}^2$ and from Gayou *et al.*[10]. for $3.5 \leq Q^2 \leq 5.5 \text{ GeV}^2$.

where the \dots represents common factors. The term $F_1 \sim \langle \uparrow \mathbf{p}'_3 | \uparrow \mathbf{p}_3 \rangle$ is a spin-non-flip term and $QF_2 \sim \langle \uparrow \mathbf{p}'_3 | \downarrow \mathbf{p}_3 \rangle$ depends on the spin-flip term. In doing the integral each of the momenta, and M_0, M'_0 can take the large value Q for some regions of the integration. Thus in the integral

$$\langle \uparrow \mathbf{p}'_3 | \uparrow \mathbf{p}_3 \rangle \sim \frac{Q}{Q}, \quad \langle \uparrow \mathbf{p}'_3 | \downarrow \mathbf{p}_3 \rangle \sim \frac{Q}{Q}, \quad (19)$$

so that F_1 and QF_2 have the same Q^2 dependence. This is shown in Fig. 1. Indeed, for Q^2 greater than about 2 GeV^2 , the ratio $\frac{QF_2}{F_1}$ varies very little with increasing Q^2 .

9 Neutron Charge Form Factor

The neutron has no charge, $G_{En}(Q^2 = 0) = 0$, and the square of its charge radius is determined from the low Q^2 limit as $G_{En}(Q^2) \rightarrow -Q^2 R^2 / 6$. The quantity R^2 is well-measured[11] as $R^2 = -0.113 \pm 0.005 \text{ fm}^2$. The Galster parameterization[12] has been used to represent the data for $Q^2 < 0.7 \text{ GeV}^2$.

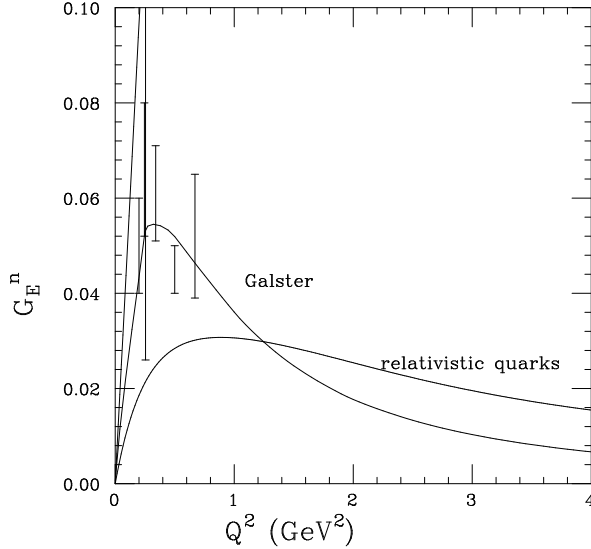


Figure 2: Calculation of G_E^n . The data are from Ref. [13], with more expected soon[14].

Our proton respects charge symmetry, the interchange of u and d quarks, so it contains a prediction for neutron form factors. This is shown in Fig. 2. The resulting curve labeled relativistic quarks is both large and small. It is very small at low values of Q^2 . Its slope at $Q^2 = 0$ is too small by a factor of five, if one compares with the straight line. But at larger values of Q^2 the prediction is relatively large.

Our model gives $R_{\text{model}}^2 = -0.025 \text{ fm}^2$, about five times smaller than the data. The small value can be understood in terms of $F_{1,2}$. Taking the definition (2) for small values of Q^2 gives

$$-Q^2 R^2/6 = -Q^2 R_1^2/6 - \kappa_n Q^2/4M^2 = -Q^2 R_1^2/6 - Q^2 R_F^2/6, \quad (20)$$

where the Foldy contribution, $R_F^2 = 6\kappa_n/4M^2 = -0.111 \text{ fm}^2$, is in good agreement with the experimental data. That a point particle with a magnetic moment can explain the charge radius has led some to state that G_E is not a measure of the structure of the neutron. However, one must include the Q^2 dependence of F_1 which gives R_1^2 . In our model $R_1^2 = +0.086 \text{ fm}^2$ which nearly cancels the effects of R_F^2 . Isgur[15] showed that this cancellation is a natural consequence of including the relativistic effects of the lower

components of the Dirac spinors. Thus our relativistic effects are standard. We need another source of R^2 . This is the pion cloud.

10 Pion Cloud and the Light Front Cloudy Bag Model

The effects of chiral symmetry require that sometimes a physical nucleon can be a bare nucleon immersed in a pion cloud. An incident photon can interact electromagnetically with a bare nucleon, a pion in flight or with a nucleon while a pion is present. These effects were included in the cloudy bag model[16], and are especially pronounced for the neutron. Sometimes the neutron can be a proton plus a negatively charged pion. The tail of the pion distribution extends far out into space (see Figs. 10 and 11) of Ref.[16], so that the square of the charge radius is negative.

It is necessary to modernize the cloudy bag model, so as to make it relativistic. This involves using photon-nucleon form factors from our model, using a relativistic π -nucleon form factor, and treating the pionic contributions relativistically by doing a light front calculation. We define the resulting model as the light-front cloudy bag model LFCBM.

The calculation is implemented by evaluating the relevant Feynman diagrams of Fig. 3 by integrating over k^- analytically (k^μ is the momentum of the emitted virtual pion) and the other three components numerically; see Ref. [3]. Thus the Feynman graphs, Fig. 3, are represented by a single τ -ordered diagram. The use of J^+ and the Yan identity[17] $S_F(p) = \sum_s u(p, s)\bar{u}(p, s)/(p^2 - m^2 + i\epsilon) + \gamma^+/2p^+$ allows one to see that the nucleon current operators appearing in Fig. 3b act between on-mass-shell spinors.

There are four model parameters: $m, \beta, \gamma, \Lambda_{\pi N}$, with $\Lambda_{\pi N}$ representing the cut-off in the pion-nucleon form factor. Including the effects of the pion cloud gives contributions to the magnetic moments of the proton and neutron, so it is necessary to re-fit the parameters. A sample of the values of the parameters is given in Table 1.

The result is termed the light front cloudy bag model[3] (even though there is no bag), and results are shown in Fig. 4. We see that the pion cloud effects are important for small values of Q^2 and, when combined with those of the relativistic quarks coming from the bare nucleon, leads to a good

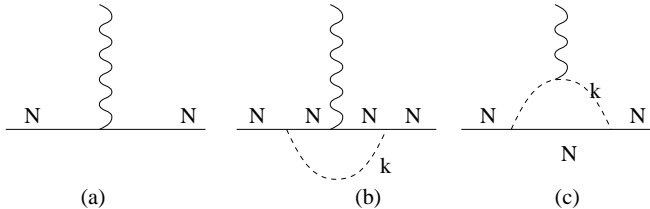


Figure 3: Diagrams. The dashed line represents the virtual pion of momentum k^μ .

Table 1: Different parameter sets, units in terms of fm

Set(legend)	m	β	Λ	γ	$-R_n^2$	$-\mu_n$	μ_p
1 solid	1.8	3.65	3.1	4.1	0.111	1.73	2.88
2 dot-dash	1.7	3.4	3.1	3.9	0.110	1.79	2.95
3 dash	1.7	2.65	3.1	3.7	0.109	1.79	2.95

description of the low Q^2 data. The total value of G_E is substantial for large values of Q^2 .

One might ask how the effects of the pion cloud influence the results shown in Fig. 1. They do not change the picture very much. The pion cloud effects influence the low momentum transfer properties, but vanish at large momentum transfer. Fig. 1 shows QF_2/F_1 which vanishes at $Q = 0$, so the influence of pion cloud effects is hidden.

We have shown one ratio and one form factor. But there are four nucleon electromagnetic form factors. The remaining two are shown in Figs. 5 and 6.

Speaking in a general fashion, I can say that good descriptions of $G_M^{p,n}$ are obtained. If one looks closely there are disagreements with the data. One sees, at very large values of Q^2 , that our value of G_M^p is too small, and this allows room for the effects of perturbative QCD [18]. that have been neglected. The wiggles at low values of Q^2 are also worthy of comment. These arise because the effects of the pion field fall off faster with increasing Q^2 than the dipole form used for comparison. Our result for G_M^n shows too deep a dip at low Q^2 in comparison with recent data[19].

The axial form factor, $G_A(Q^2)$ is not calculated here. Schlumpf's model

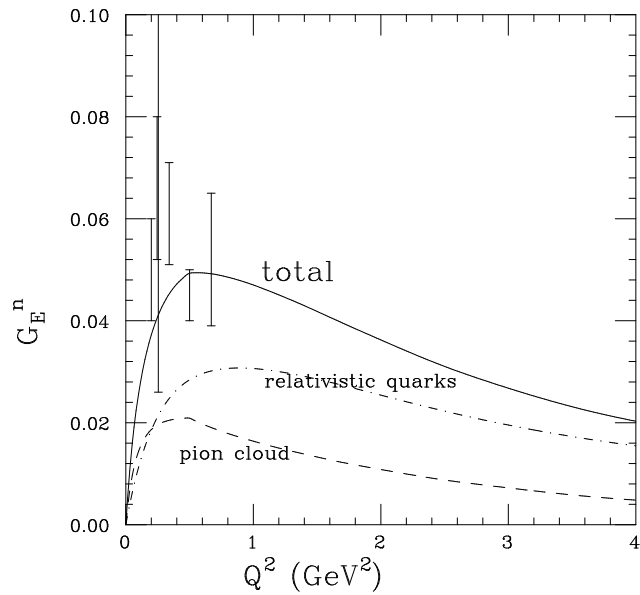


Figure 4: Light front cloudy bag model LFCBM Calculation of G_E^n [3].

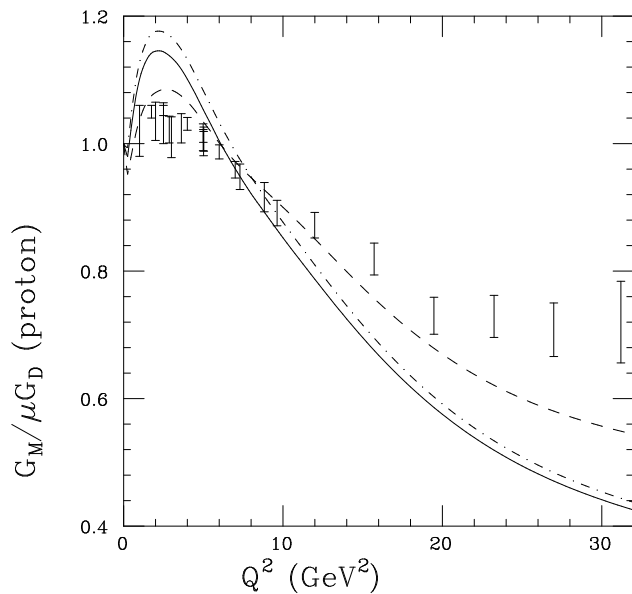


Figure 5: Light front cloudy bag model LFCBM Calculation of G_M^p [3].

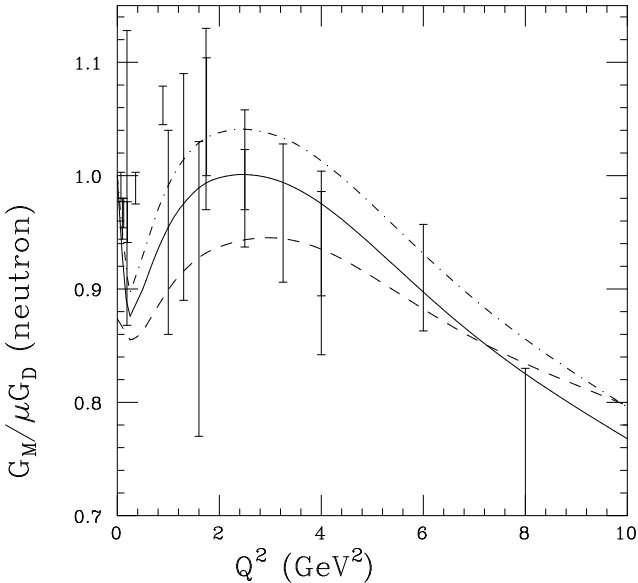


Figure 6: Light front cloudy bag model LFCBM Calculation of G_M^n [3].

obtained an excellent reproduction of existing data[6], and our parameters are similar to his. The lowest-order effect of the pion cloud vanishes, so the principal difference between G_A of our model and that of Ref. [6] is that our quark masses have larger values. This increases the computed value of g_A for a bare nucleon by about 10 – 15%. But this is opposed by the need to multiply the bare nucleon result by the renormalization factor Z of about 0.85 – 0.9. Thus our results for $G_A(Q^2)$ should be similar to those of [6].

11 Summary

These calculations show that the combination of Poincaré invariance and pion cloud effects, is sufficient to describe the existing experimental data up to about $Q^2 = 20$ GeV^2 . This is somewhat surprising as the model keeps only two necessary effects. Configuration mixing of quark[20], the variation of the quark mass with Q^2 [21], exchange currents[22] and an intermediate Δ [16] have not been included. These effects either have modest influence, are incorporated implicitly through the choice of parameters, or will help to remove any remaining differences with experiment.

Acknowledgements

I thank the USDOE for partial support of this work.

References

- [1] M.R. Frank, B.K. Jennings and G.A. Miller, Phys. Rev. C **54**, 920 (1996).
- [2] G. A. Miller and M. R. Frank, Phys. Rev. C **65**, 065205 (2002)
- [3] G. A. Miller, Phys. Rev. C **66**, 032201 (2002) [arXiv:nucl-th/0207007].
- [4] V. B. Berestetskii and M. V. Terent'ev. Sov. J. Nucl. Phys. **25**, 347 (1977).
- [5] P. L. Chung and F. Coester. *Phys. Rev. D* **44**, 229, (1991).
- [6] F. Schlumpf, U. Zurich Ph. D. Thesis, hep-ph/9211255.
- [7] P. Jain, B. Pire and J. P. Ralston, Phys. Rept. **271**, 67 (1996) ; T. Gousset, B. Pire and J. P. Ralston, Phys. Rev. D **53**, 1202 (1996)
- [8] V. M. Braun, A. Lenz, N. Mahnke and E. Stein, Phys. Rev. D **65**, 074011 (2002).
- [9] M. K. Jones *et al.* [Jefferson Lab Hall A Collaboration], Phys. Rev. Lett. **84**, 1398 (2000) [arXiv:nucl-ex/9910005].
- [10] O. Gayou, E. J. Brash, M. K. Jones, C. F. Perdrisat and V. Punjabi, Phys. Rev. Lett. **88**, 092301 (2002)
- [11] S. Kopecky *et al.*, Phys. Rev. Lett. **74**, 2427 (1995)
- [12] S. Galster *et al.*, Nucl. Phys. B **32**, 221 (1971).
- [13] T. Eden *et al.*, Phys. Rev. C **50**, 1749 (1994); M. Meyerhoff *et al.*, Phys. Lett. B **327**, 201 (1994); M. Ostrick *et al.*, Phys. Rev. Lett. **83**, 276 (1999). J. Becker *et al.*, Eur. Phys. J. A **6**, 329 (1999). I. Passchier *et al.*, Phys. Rev. Lett. **82**, 4988 (1999) D. Rohe *et al.*, Phys. Rev. Lett. **83**, 4257 (1999). H. Zhu *et al.* Phys. Rev. Lett. **87**, 081801 (2001)

- [14] Jefferson Laboratory Experiment 93-038, R. Madey Spokesperson; R. Madey, for the Jlab E93-038 collaboration, “Neutron Electric Form Factor Via Recoil Polarimetry”, contribution to Baryons 2002.
- [15] N. Isgur, Phys. Rev. Lett. **83**, 272 (1999)
- [16] S. Théberge, A. W. Thomas and G. A. Miller, Phys. Rev. **D22** (1980) 2838; (1981) 2106, A. W. Thomas, S. Théberge, and G. A. Miller, Phys. Rev. **D24** (1981) 216; S. Théberge, G. A. Miller and A. W. Thomas, Can. J. Phys. **60**, 59 (1982). G. A. Miller, A. W. Thomas and S. Théberge, Phys. Lett. B **91**, 192 (1980).
- [17] S. J. Chang and T. M. Yan, Phys. Rev. D **7**, 1147 (1973).
- [18] G. P. Lepage and S. J. Brodsky, Phys. Rev. D **22**, 2157 (1980).
- [19] W. Xu *et al.*, Phys. Rev. Lett. **85**, 2900 (2000); G. Kubon *et al.*, Phys. Lett. B **524**, 26 (2002)
- [20] F. Cardarelli and S. Simula, Phys. Rev. C **62**, 065201 (2000)
- [21] J. C. Bloch, C. D. Roberts, S. M. Schmidt, A. Bender and M. R. Frank, Phys. Rev. C **60**, 062201 (1999); C. D. Roberts, and S. M. Schmidt, Prog. Part. Nucl. Phys. **45**, S1 (2000).
- [22] W. R. de Araujo, E. F. Suisso, T. Frederico, M. Beyer and H. J. Weber, Phys. Lett. B **478**, 86 (2000); E. F. Suisso, W. R. de Araujo, T. Frederico, M. Beyer and H. J. Weber, Nucl. Phys. A **694**, 351 (2001); K. Bodoor, H. J. Weber, T. Frederico and M. Beyer, Mod. Phys. Lett. A **15**, 2191 (2000)